XVIII IMEKO WORLD CONGRESS
Metrology for a Sustainable Development
September, 17 – 22, 2006, Rio de Janeiro, Brazil

THERMAL MICROSENSOR FOR APPLICATION IN RADIOMETER

Francisco Santos[1], *Rafael Cantalice,*[1]*Raimundo Freire*[1], *Will Almeida, Elmar Melcher*[1],

[1]UFCG-CCT-DEE, LIMC, Campina Grande, PB, Brazil, ffsantos @dee.ufcg.edu.br, rcsfreire@dee.ufcg.edu.br, Elmar @dee.ufcg.edu.br, willalmeida@dee.ufcg.edu.br, rafaelcantalice@gmail.com

Abstract: In this paper presents two microsensors structures compatible with microelectronic technologies that are analyzed for application in radiometers. The first structure is formed by one resistor that is made by doping a monocrystalline silicon substrate with boron. The second is a polysilicon resistor doped with phosphorous, over a silicon dioxide (SiO2). The analysis is made by mathematical modeling of these devices, numeric simulation and graphics to obtain the better thermal-electrical characteristic of microsensor material. We choose the best microsensor structure with the increase performance of the system and with time decrease of sensor thermal response in relation the conventional manufacture for application in incident solar radiation measurement.

Keywords: thermal microsensor, radiometer, polysilicon resistor.

1. INTRODUCTION

Sensors, whose operation base is the heat transfer, calls of thermal sensors, are used in many applications, as: temperature measurement, humidity, flow, radiation, gases thermal conductivity, temperature control [1-6]. The fabrication technologies applied for silicon microsensors use materials and processes borrowed from the IC technology. These standard process steps allow batch fabrication of microsensors similar to the integrated circuits fabrication. The great variety of applications that use microsensor as thermal sensor justifies the studies on the same.

The thermal-electrical model of microsensor structures is validated by the results of the numeric simulation. As results are presented: the isolation influence of the resistor in the temperature distribution, the thermal and electrical material conductivities influences on microsensors temperature distribution, resistance variation and power density relations, dopant concentration resistance influence on the polysilicon resistor TCR (temperature coefficient of resistivity) and power consumption. The analysis evaluate the types of structures used with and without isolation of the resistor, based on the thermal and electrical materials conductivities influences, with the objective of knowing which the structure is the best to apply as sensor. We choose the better linear model in order to evaluate the response of the thermal and electrical variations of device and to optimize the parameters that influences in the linearity.

With this there are the fabrication possibilities of several planar geometries and thermal microsensors simultaneous with electronic circuits in CMOS with good performance.

2. THERMAL MICROSENSOR

The thermal microsensor was modeled with base in two structures types. In the fig.1 represents the microsensor monocrystalline doped with boron in which his extremity is on the silicon surface. The fig.2 represents the microsensor polycrystalline in which his extremity is on silicon dioxide (SiO_2). The triangles in each one of the figures form the *mesh* defined by the software, which calculates the variables of the problem in each one of the vertexes.

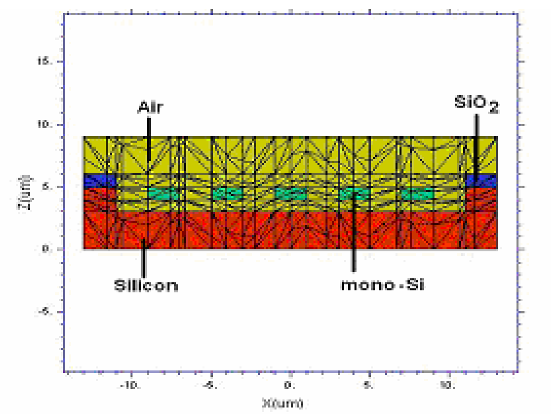

Fig.1. Thermal microsensor of monocrystalline silicon

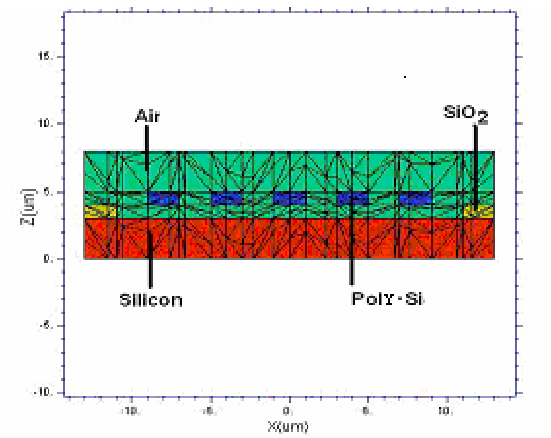

Fig. 2. Thermal microsensor of polycrystalline silicon

It is observed that the two structures have as base a resistor in bridge, forming a membrane as in the fig. 3.

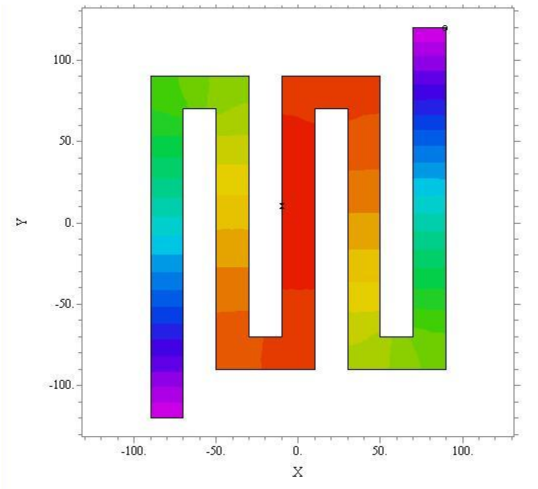

Fig. 3. Thermal microsensor

The physical dimensions of the microsensor are: Width: 20 µm, Thickness: 0.5 µm, Length: 1040 µm.

The structures were simulated by systems resolution of partial differential equations due to no linearity of the equations

2.1. Equations:

The mathematical model of the domains thermal and electrical of the microsensor is based on the following equations.

The equation that is based the thermal domain is the current continuity equation:

$$\nabla.\vec{J} = -\frac{\partial \rho_e}{\partial t} \qquad (1)$$

The relations among the current density, electric field $\vec{E}$ and potential electric V are defined by the equations:

$$\vec{j} = \sigma(x,y,z,T)\vec{E} \qquad (2)$$

$$\vec{E} = -\nabla V \qquad (3)$$

Considering that the conductivity is uniform in all material and that the sensor operates in permanent regime, with the equations 1, 2 and 3 we arrived to the main equation of the electric domain:

$$\nabla\sigma(T)\nabla V + \sigma(T)\nabla^2 V = 0 \qquad (4)$$

The thermal behavior of the device is determined by the continuity equation of the heat flow:

$$Q = \nabla.\vec{f} + h\left(T - T_\infty\right) + \varepsilon\sigma\left(T^4 - T_\infty^4\right) + \rho_m C_p \frac{\partial T}{\partial t} \qquad (5)$$

The term Q is an internal heat source to the device. This heat source can be generated by several physical phenomena: electric (Joule effect), mechanics, chemical, and others. The first term on the right side of that equation represents the change of heat by thermal conduction, the second, by convection, the third party, by radiation. The fourth term is the variation interns of temperature in the device.

To make resistors with linear characteristic between resistivity and temperature, a semiconductors model was used highly doped, and that, as larger the dopant, more linear this relation. It is possible to get an approximate relation for a first order polynomial by:

$$\rho(T) = \rho_0\left[1 + \alpha\left(T - T_0\right)\right] \qquad (6)$$

The first step for the structure simulation is the definition of its geometry and of the materials that compose. That is made attributing the thermal properties and electrical characteristics of a material to its specific area in the volume that limits the device.

2.2. Thermal and Electrical Conductivities of the Materials for Simulation

The areas that compose each material were defined based on the thermal and electrical properties of each one. In the Table 1 are shown the values from each material used in the simulations, where is possible to analyze the effect of the thermal conductivity of the materials in the temperature distributions in the structures.

Table 1 - Thermal and Electrical Conductivities of the Materials for Simulation

Material	**Thermal Conductivity (W/mK) [7]**	**Electrical Conductivity (Ω-1)**
Monocrystalline Silicon (substrate type N)	148	$4\ x10^{-2}$
Monocrystalline Silicon (doped with Boron)	148	$4\ x10^{-5}$
Polycristalline Silicon	32 [8]	$4\ x10^{-2}$
Silicon Dioxide	1.38	$4x10^{-7}$
Air	0.0263	$4\ x10^{-7}$

After the definition of the microsensor geometry, it is necessary to apply voltage and temperature. In the simulation, that is made based on conditions applied to the necessary areas. As the problem to be solved has two variables, is necessary to supply the conditions for each one of them [9].

2.3. Thermal Simulation

The temperature distribution of the structures is shown in the fig. 3 and 4, corresponding to the microsensor of silicon monocrystalline and polycrystalline, respectively.

As parameters considered in the simulation: the resistor with an initial temperature of 25 °C and a voltage of 1V in their terminals.

The temperature distribution along the resistor is shown in the fig. 3. The increase in the isolation thermal decreases the heat loss of the resistor to the substrate, what provokes an increase in the temperature of the device, which is of approximately 47 °C. Besides, the temperature decreases in the direction of the resistor center to their extremities, through where the substrate absorbs heat of the resistor.

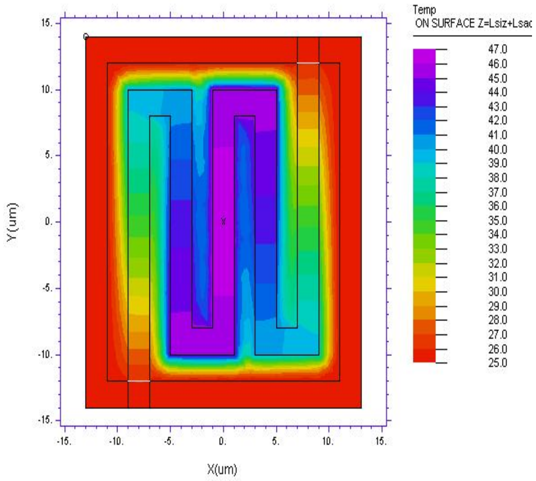

Fig. 3. Temperature Distribution in the microsensor monocrystalline

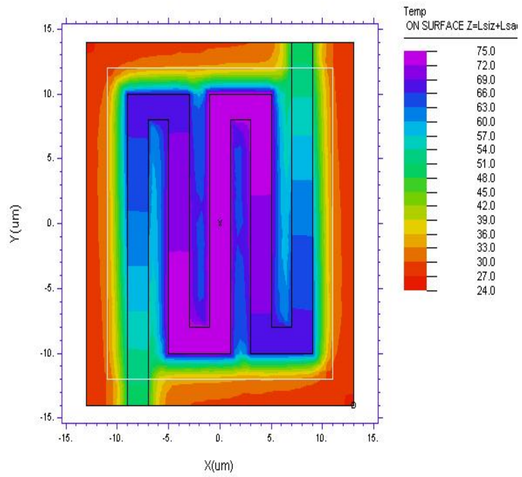

Fig. 4. Temperature Distribution in the microsensor polycrystalline

In the fig. 4 the maximum temperature in the microsensor increases until approximately 75 °C, and this temperature is not uniformly distributed, tends a maximum value in the center of the microsensor and decreasing in direction their extremities. The significant increase of temperature is due to the best thermal isolation of the microsensor. Since the air is less conductive thermal that the silicon dioxide (see Table 1), there is a smaller heat loss of the device for the substrate.

Due to the characteristics of the microsensor formed by the resistor polycrystalline to offer better isolation, consequently bigger sensivity, we did the other part of the simulation with a more detailed study of the thermal-electrical characteristics. In that part, the simulations are made just considering the resistor.

2.4. Thermal and Electrical Simulation

In this section the thermal-electrical simulations of the devices is presented. The obtained results are the relations curves between electrical current and applied voltage, resistance in function of the voltage, and potency dissipated in the devices.

The conductivity of the resistor is controlled by the dopants concentration in the polycrystalline silicon, considering that resistor has a resistivity equal the 25 Ω.µm. Experimentally was proven that this conductivity can be obtained with a phosphorous implantation with dose of $7x10^{15}$ atoms/cm^2 and energy of 150 keV. It should be taken into account TCR, which will be considered equal to 1500 ppm/°C [10].

In this simulation is applied to the device a voltage of 1 V, but this voltage should be increased in small intervals, in the order of 0.1 V, so that happens convergence in the simulation. With this, 10 iterations of 0.1 V, and the result of each one them is considered as initial condition for the following. This low voltage value was due to the time of simulation to be very big for each iteration. For each iteration generates a summary, where the values of some selected variables are presented.

In the Table 2 is shown the summary of the first simulation iteration, for a voltage of 0.1 V, and of the last iteration, for a voltage of 1 V. Important information is the resistance for each one of these voltages. For the 0.1V voltage the resistance is of 2.6039 KΩ, while in the voltage of 1 V the resistance increases for a value of 2.942 KΩ, due to the potency dissipation.

Table 2. Summary of the iterations

Voltage [V]	0,1	1
Resistance[Ω]	2603.9	2942.5
Current [mA]	$3.84x10^{-2}$	$3.398x10^{-1}$
Potency [W]	$3.84x10^{-6}$	$3.398x10^{-4}$
Potency Density [W/µm^3]	$3.69x10^{-10}$	$3.26x10^{-8}$

In the fig. 5 the Resistance x voltage curve is shown. It is observed the increase of the resistance clearly with the increase of the applied voltage. For a resistance Variation of 2.6039 to 2.942 KΩ. We have a voltage of 0.1 to 1 V.

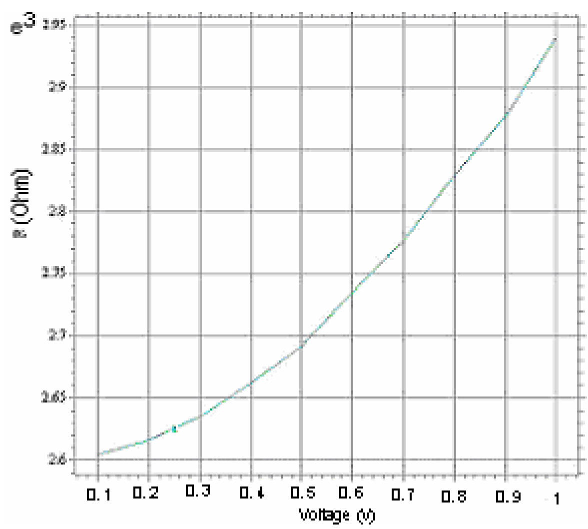

Fig. 5. Resistance x Voltage

The Current x Voltage curve is shown in the fig. 6; the inclination of this is also an indicative of the resistance increase.

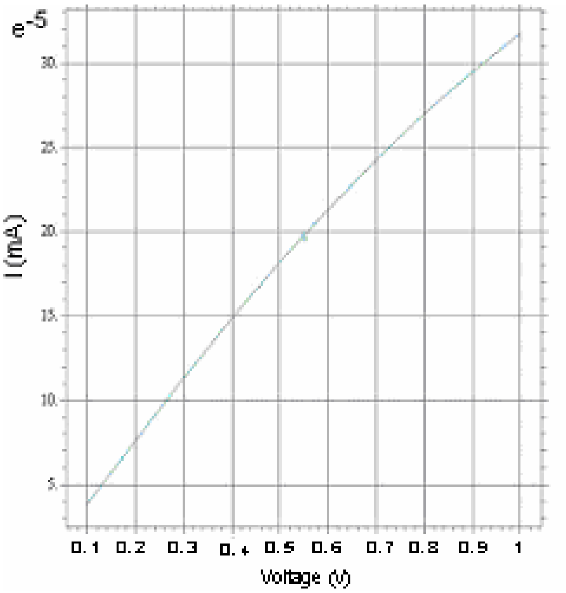

Fig. 6. Current x Voltage

We observed in a certain way a low consumed potency, which is due to the fact that we just considered the resistor structure in the simulation, soon the resistor doesn't lose heat for the substrate, every applied voltage in it just influences in its temperature increase.

2.5. Simulation in measurement of solar radiation

In the simulation we just considered the resistor, disrespecting the losses for the structure. The resistor in the simulation was considered as one laminates due to its thickness to be much smaller than their other dimensions.

The equations 5 and 6 are used to solve this problem just considering the heat change with the environment by radiation, (without convection and conduction), and with the heat generated due the voltage and distribution of heat in the resistor

The simulation of the microsensor in measurement solar radiation was accomplished considering the following parameters: the thermal conductivity 148 W/mK, emissivity of the resistor 0.64, the incident solar radiation band variation considered was from 0 to 1500 Watts/m^2 (that is the maximum intensity of radiation received in the terrestrial surface close to the equator), an initial temperature of 25 °C and a voltage of 100mV in their terminals.

The linear characteristic between the resistance of the sensor and its maximum temperature is presented in the fig. 7. This curve represents the linear relationship between the resistance and temperature for a silicon resistor highly doped, as mentioned in previously. And the resistance increases of 5.210 KΩ to 5.255 KΩ considering a temperature of 25 ° C to 115 °C.

It is shown in the fig. 8 the linear characteristic between the resistance of the sensor and the solar radiation. For a resistance variation of 5. 210 KΩ until 5.255KΩ we have an incident solar radiation (H) of 0 to 1500 Watts/m^2.

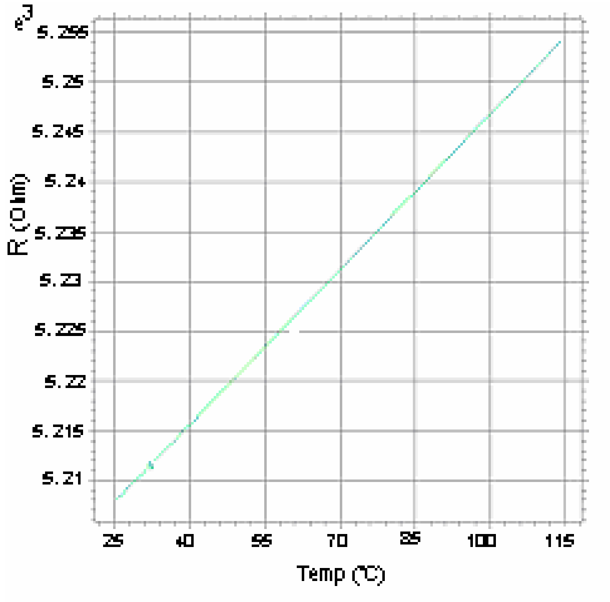

Fig. 7. Resistance x Temperature

Those results indicate the possibility to build a sensor for solar radiation measurement using this structure type, but it is important to comment that relationship between the resistance and the solar radiation was obtained being applied a constant voltage (CV) to the resistor. Most of the sensor operates in constant temperature (CT), obtained by the use of feedback circuits.

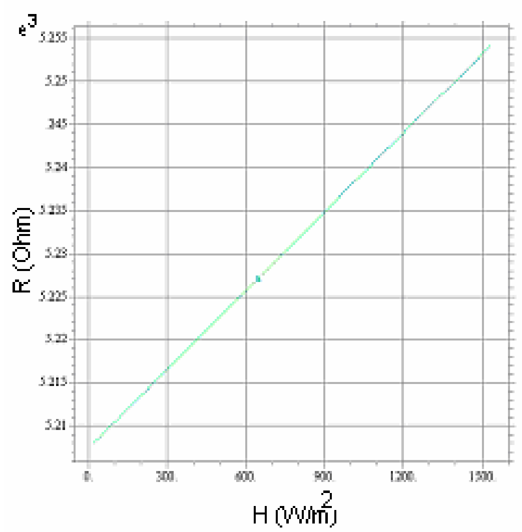

Fig. 7. Resistance x Solar Radiation

3. CONCLUSION

The results of the accomplished simulations are of great importance for the understanding and forecast of the thermal and electrical characteristics of the microsensor, because we can prove such characteristics for the temperature distributions of each structure and to analyze which the structures that offer better results to work as sensor thermal.

In the simulations was verified that the devices with the polycrystalline silicon resistor present an efficiency of larger heating than the simulated ones in the silicon substrate, due to the use of the silicon oxide as insulating thermal, stiller guaranteeing the resistor isolation due to the material to consume less potency than the substrate.

It is observed in the simulations done in the resistors that the relative variation of the resistance is controlled by the electrical potency dissipated density by the resistor. With that intuitively we can affirm that for the device of the microsensor that variation is also verified.

About the production processes, there would not be any difficulty in including other together electronic devices to the microsensor, since the stages of the processes they allow the simultaneous production of these devices.

ACKNOWLEDGMENTS

The authors acknowledge the CNPq (Conselho Nacional de Desenvolvimento Cientìfico e Tecnológico) and CAPES/ PROCAD (Coordenação de Aperfeiçoamento de Pessoal do Ensino Superior), for the financial support and award of fellowships during the period of this work.

REFERENCES

[1] Wu, Y.E., Chen, K., Chen, C.W., Hsu, K.H., "Fabrication and characterization of thermal conductivity detectors (TCDs) of different flow channel and heater designs", Sensors and Actuators A 100, , 37-4591, 2002.

[2] Schmid, U., "A robust flow sensor for high pressure automotive applications", Sensors and Actuators A 97-97, 253-263, 2002.

[3] Abedinov, N., Grabiec, P., Gotszalk, T., Ivanov, Tz, Voigt, J., Rangelow, I.W., "Micromachined piezoresistive cantilever array with integrated resistive microheater for calorimetry and mass detection", J. Vac. Sci. Technol. A, 19 (6), 2884-2888, 2001.

[4] Park, H., Pak, J.J., Son, S.Y., Lim., G., Song, I., "Fabrication of a microchannel integrated with inner sensors and the analysis of its laminar flow characteristics", Sensors and Actuators A 103, , 317-329, 2003.

[5] Kajiyama, T., Miyahara, Y., Kricka, L. J., Wilding, P., Graves, A. J., Surrey, S., Fortina, P., "Genotyping on a Thermal Gradient DNA Chip", Genome Res. 13: 467-475, 2003.

[6] Doebelin. E. O, "Measurement Systems. Application and Design", 4th ed., New York: McGraw-Hill Co., 1990.

[7] Rossi, C., Temple-Boyer, P., Estève, D., "Realization and performance of thin SiO2/SiNx membrane for microheater applications", Sensors and Actuators A 64 (1998) 241-245

[8] Das, N. C., Monroy, C., Robinson, D., Jhabvala, M., "Design and fabrication of low power polysilicon sources", Solid-State Electronics 43 (1999) 1239-1244

[9] Adeilton Junior, C. de Oliveira, "Development of Microheaters compatible with Technologies of Microelectronic for Application in Thermal Transducers", Master's degree dissertation, UNICAMP-Campinas, September 2003.

[10] Boukabache, A., Pons, P., "Doping effects on thermal behavior of silicon resistor", Electronics Letters, 2002, 38, 7, pp. 342-343